Co-ordinated modulation of Ca^{2+} and K^+ currents during ascidian muscle development

Adrienne A. Greaves, Anna K. Davis, Julia E. Dallman and William J. Moody*

Department of Zoology, Box 351800, University of Washington, Seattle, WA 98195, USA

1. The development of Ca^{2+} and K^+ currents was studied in ascidian muscle cells at twelve embryonic stages from gastrulation to the mature cell, a period of 24 h. A high degree of co-ordination occurs between the development of the inwardly rectifying K^+ current ($I_{K(IR)}$), which sets the resting potential, and Ca^{2+} and outward K^+ currents, which determine action potential waveform.

2. At neurulation $I_{K(IR)}$, which had been present since fertilization, begins to decrease, reaching 12% of its previous density in 6 h. $I_{K(IR)}$ then immediately begins to increase again, reaching its previous density in another 6 h.

3. When $I_{K(IR)}$ begins to decrease, a high-threshold inactivating Ca^{2+} current and a slowly activating voltage-gated K^+ current appear.

4. When $I_{K(IR)}$ returns to its previous density, two new currents appear: a sustained Ca^{2+} current with the same voltage dependence, but different conotoxin sensitivity than the inactivating Ca^{2+} current; and a Ca^{2+}-dependent K^+ current, which activates 8–10 times faster and at potentials 20–30 mV more negative than the voltage-dependent K^+ current.

5. The transient downregulation of $I_{K(IR)}$ destabilizes the resting potential and causes spontaneous action potentials to occur. Because $I_{K(IR)}$ is absent when only a slowly activating high-threshold outward K^+ current is present, these action potentials are long in duration.

6. The return of $I_{K(IR)}$ and the appearance of the rapidly activating Ca^{2+}-dependent K^+ current eventually terminate this activity. The action potentials of the mature cell occur only on stimulation, and are 10 times shorter in duration than those in the immature cell.

The ion channels expressed early in the development of excitable tissue are often markedly different from those found in the mature cells. In some cells, this difference takes the form of Ca^{2+} currents that are larger relative to the Na^+ current than later in development, and outward K^+ currents that are smaller and slower, resulting in action potentials that are longer in duration and more Ca^{2+} dependent than in the mature cell (Barish, 1986; O'Dowd, Ribera & Spitzer, 1988). In other cells, the differences are more subtle, changing the ratio of inward currents to repolarizing or resting conductances, so that the immature cell is more excitable, or fires action potentials in a different pattern than the mature cell (e.g. Linsdell & Moody, 1995). In extreme cases, channels involved in generating the action potential may be present only at early stages of development, so that the cell loses its excitability during maturation (e.g. Sontheimer, Trotter, Schachner & Ketterman, 1989; Barres, Koroshetz, Swartz, Chun & Corey, 1990; for reviews see Moody, Simoncini, Coombs, Spruce & Villaz, 1991; Spitzer, 1991; Moody, 1995).

The idea that these differences reflect a developmental role for spontaneous action potentials has now gained wide acceptance. Spontaneous activity has been shown to mediate many developmental events in nerve and muscle, such as axonal pathfinding and expression of mature forms of ion channels and contractile proteins (Cerny & Bandman, 1986; Holliday & Spitzer, 1990; Shatz, 1990; Dutton, Simon & Burden, 1993; Linsdell & Moody, 1995). Studies using specific misexpression of ion channels have confirmed that the precise pattern of channel expression at early stages is essential for spontaneous activity to mediate such processes accurately (Jones & Ribera, 1994; Linsdell & Moody, 1994).

However, the channels that bring the cell to threshold and trigger such activity are likely to be different from those that govern the waveform of the action potential itself. Therefore, for spontaneous action potentials to play a role in development, the events that trigger them must be co-ordinated with the development of the channels that ensure their appropriate, immature waveform and ionic

* To whom correspondence should be addressed.

All authors have contributed equally to this work.

dependence. This paper reports the results of a study of Ca^{2+} and K^+ current development in ascidian muscle which reveals that such co-ordination can occur by linking the development of an inwardly rectifying K^+ current, which sets the resting potential, to that of the Ca^{2+} and outward K^+ currents, which control spike duration. Ascidians are marine chordates whose rapid development, early commitment of cell fates, and small cell number make them ideal for the study of the development of excitable tissue (Satoh, 1994). Muscle-lineage cells of the species we have used contain an orange pigment that allows them to be identified at all developmental stages, even before they express overt morphological characteristics of muscle (see Simoncini, Block & Moody, 1988). Our previous work on these cells (Davis, Greaves, Dallman & Moody, 1995) showed that after the muscle-lineage cells complete their terminal cell division at the neurula stage, they downregulate the inwardly rectifying K^+ current that was present at earlier stages, and express a small, high-threshold inactivating Ca^{2+} current and a small, slowly activating delayed K^+ current. In the mature state, these cells re-express the inward rectifier, express both a large, high-threshold sustained Ca^{2+} current and a large outward K^+ current, which is rapidly activating and partially calcium dependent. (Ascidian muscle cells have no Na^+ current, and their contraction depends on Ca^{2+} entry during the action potential.)

In this paper, we show that the window of time during which the inward rectifier is absent and spontaneous activity is likely to occur, is very short and is the same window during which the cells have only a high-threshold slowly activating delayed K^+ current. This ensures that spontaneous action potentials are long in duration and can admit significant amounts of calcium. Using current-clamp recordings, we show that spontaneous, long-duration action potentials do indeed occur during this window. At the end of this window, the appearance of a Ca^{2+}-dependent K^+ current, whose rapid activation kinetics speed the activation of the total outward K^+ current by about 10-fold, is coincident with the return of the inward rectifier. These events serve both to shorten the duration of action potentials and to prevent their spontaneous occurrence.

METHODS

Animals

Boltenia villosa were collected from Puget Sound and maintained in sea water at 11 °C with constant light to discourage spawning. To harvest gametes, animals were placed in iced sea water and then killed by a rapid cut, which bisected the siphons in the area of the cerebral ganglion, and gametes were removed with forceps. Procedures for fertilizing eggs and rearing embryos were as previously described (Block & Moody, 1987), with the modification that, in later experiments, gonads from two animals containing both eggs and sperm were minced together through 220 μm nylon mesh, rather than separating the eggs and sperm from each animal and cross-fertilizing. Self-fertilization may occur using this method, but we have noted no developmental abnormalities.

Solutions

Bath solutions. Normal artificial sea water (ASW) contained (mM): 400 NaCl, 10 KCl, 10 $CaCl_2$, 50 $MgCl_2$, and 10 Hepes; pH 8·0 with NaOH. Divalent-free ASW (DF-ASW) contained (mM): 460 NaCl, 10 KCl, 10 Hepes, and 5 EGTA; pH 8·0 with NaOH. Zero calcium ASW (0 Ca-ASW) contained (mM): 400 NaCl, 10 KCl, 60 $MgCl_2$, 5 EGTA and 10 Hepes; pH 8·0 with NaOH. In CAPS-buffered ASW, 10 Hepes was replaced by 10 CAPS buffer (3-(cyclohexylamino)-1-propanesulphonic acid), and the pH was adjusted to 10·0 with NaOH. Pronase-ASW contained 1 mg ml^{-1} Pronase E (Sigma) in CAPS-buffered ASW.

Internal (pipette) solutions. Normal internal solution contained (mM): 200 KCl, 10 NaCl, 1 $MgCl_2$, 1 EGTA, 20 Hepes, 2 MgATP, 0·1 cAMP, and 400 *d*-sorbitol; pH 7·3 with KOH. To block outward K^+ currents, KCl was replaced with equimolar CsCl and the pH adjusted with CsOH. Sorbitol was added to make internal solutions isosmotic with sea water. Nystatin was added to internal solutions just before recording by diluting a stock solution of nystatin (30 mg ml^{-1} in DMSO, stored at −20 °C for up to 1 week) into internal solution to a final concentration of 300 μg ml^{-1}. The pipette tip was filled with non-nystatin internal solution and then backfilled with nystatin-containing internal solution.

Dissociation of embryos

All steps of the dissociation were performed at 12 °C. Embryos normally develop within an acellular chorion. To isolate muscle cells, the chorion was removed manually with electrolytically sharpened tungsten needles in DF-ASW. Embryos were incubated in Pronase-ASW for 5–30 min, then transferred to DF-ASW for 5–40 min before gentle trituration to isolate single cells. Cells were gradually transferred back to ASW for recording, and all recordings were made within 8 h of dissociation. A control dish of undissociated embryos was kept at the same temperature and used to determine the stage of the dissociated cells as they developed during the recording session. To ensure that dissociated cells developed on approximately the same time schedule as those in the intact animal, we measured capacitance (C_m), density and activation time constant (τ_K) of the outward K^+ current (+60 mV), and density of the inwardly rectifying K^+ current from cells dissociated at the neurula stage and cultured until control animals hatched (18 h later) and from cells acutely dissociated from hatched tadpoles. None of these parameters was significantly different in the two groups: C_m, 18 ± 0·5 pF (cultured) *vs.* 20 ± 0·4 pF (acute); I_K density, 247 ± 19 pA pF^{-1} *vs.* 256 ± 18 pA pF^{-1}; τ_K, 7 ± 0·3 ms *vs.* 8 ± 1 ms; $I_{K(IR)}$ density, 7 ± 0·9 pA pF^{-1} *vs.* 5 ± 1 pA pF^{-1} (means ± S.E.M.; n.s., Student's unpaired *t* test).

Electrophysiological methods

All voltage- and current-clamp data were collected using the perforated patch configuration of the whole-cell clamp technique to reduce washout of calcium currents (Horn & Marty, 1988; cAMP and MgATP in the pipette solution were probably not necessary, but were retained from earlier experiments using conventional whole-cell recording). All recordings were performed at 12 °C. Pipettes for whole-cell clamp were pulled from 50 μl haematocrit glass to resistances of 1–4 MΩ (in ASW) using a Narishige two-stage puller. Data were filtered at 0·5 kHz (8-pole Bessel filter) and acquired at 2 kHz using pCLAMP software. Series resistance was compensated electronically and was never greater than 15 MΩ. Leakage currents, when present, were subtracted during analysis. Dissociated muscle cells are approximately spherical at all stages, with an apparent specific capacitance near 1 $\mu F\,cm^{-2}$, so they should present no space-clamp problems. We evaluated the

adequacy of voltage clamp in each cell by the rapid settling of capacitative transients and by the smooth rise of the current–voltage (I–V) relations of inward currents to their peaks. Deviation from these criteria were readily apparent, for example, when we clamped one of a coupled pair of muscle cells. Current density was calculated by dividing current amplitude by cell capacitance, which was measured as described previously (Moody & Bosma, 1985). The average capacitance of the cells increased gradually during development (tailbud stage: 16·4 ± 0·7 pF, $n = 18$; tadpole: 19·6 ± 0·4 pF, $n = 28$; $P < 0{\cdot}0002$). All measurements are presented as means ± S.E.M.

For current-clamp experiments, patch permeabilization was done under voltage clamp, with the holding potential set to −60 mV. When series resistance and capacitative transients had stabilized, the patch-clamp amplifier was switched to current clamp and the resting potential and any spontaneous activity in the absence of applied current were noted. Current was then applied to hold the resting potential near −60 mV. Action potentials were recorded after the termination of brief current pulses and during polonged current pulses. Data were accepted only if the input resistance was > 4GΩ, measured under voltage clamp as the reciprocal slope conductance between −60 and −50 mV.

Developmental stages

Between late gastrula and the hatched tadpole, we have defined twelve stages which are both reasonably equally spaced in time (~2 h intervals) and easily distinguishable by morphological criteria. Photographs of selected stages are shown in Fig. 1. Gastrula (12 h after fertilization at 12 °C) is defined by the presence of the blastopore. Late gastrula (Fig. 1; LGast, 14 h) is defined as the stage when the blastopore has narrowed to an oblong slit. The next stage, neurula (Fig. 1; Neur, 16 h) is identified by the formation and closing of the neural tube. Early tailbud (18 h) begins when the

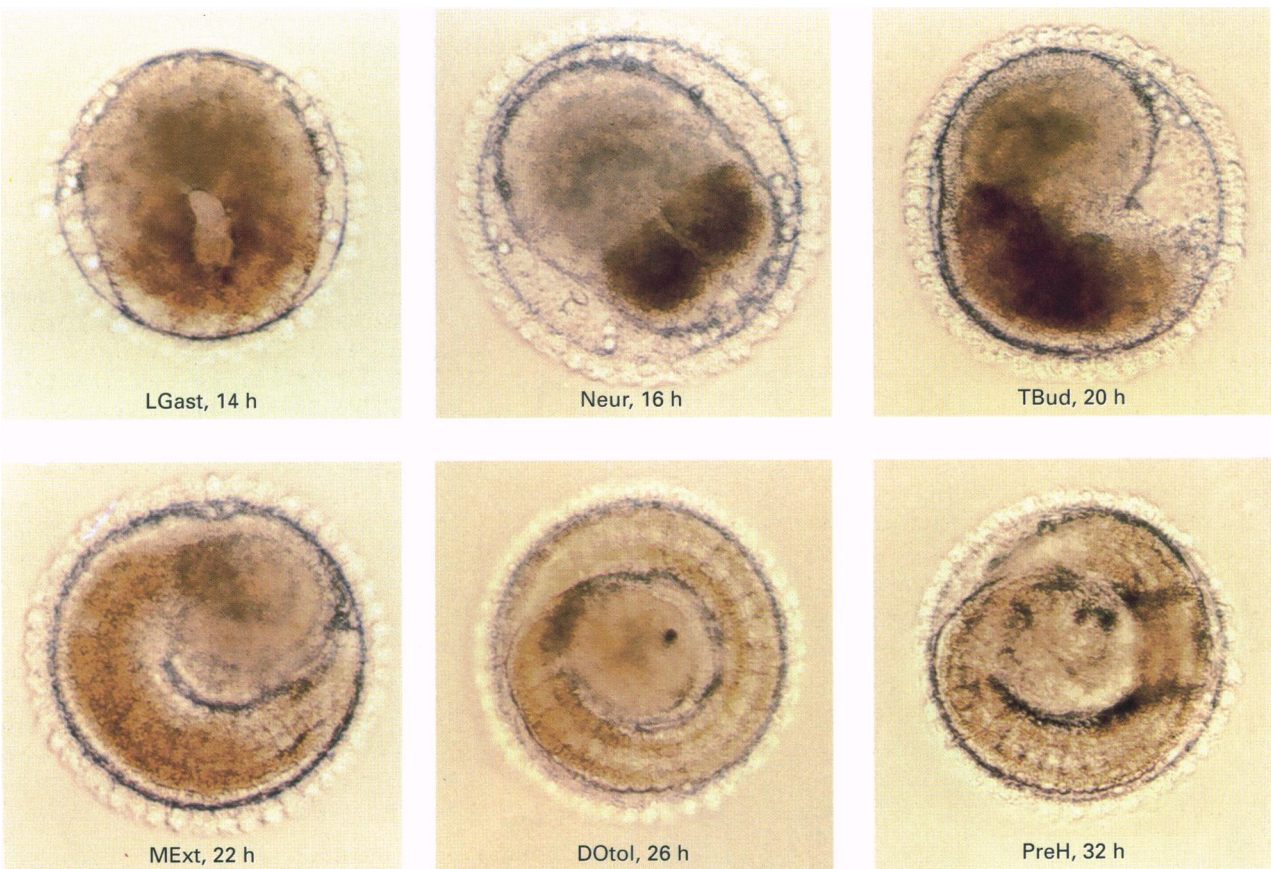

Figure 1. Photographs of *Boltenia villosa* embryos at selected developmental stages

Labels indicate the abbreviated stage name and the hours after fertilization (see Methods). All the embryos are in their acellular chorion which is surrounded by a layer of follicle cells, which are more or less clearly visible depending on the plane of focus. In the top three panels test cells can also be seen within the chorion. The diameter of the embryo and chorion is approximately 120 μm. LGast, 14 h: late gastrula, posterior-dorsal view, showing the elongated blastopore. Neur, 16 h: neurula, dorsal view; the neural tube, almost closed, can be seen running from the centre of the photograph toward the lower right, surrounded by dark orange muscle cells. TBud, 20 h: tailbud; this and all subsequent views are from the right side of the embryo. The tail has extended sufficiently to begin to bend within the chorion. MExt, 22 h: mid-extension; the tail has curled around to meet the head within the chorion. DOtol, 26 h: dark otolith; the otolith, the first of two sensory organs to appear in the head, is visible and dark. PreH, 32 h: pre-hatch; the tail has extended completely and the second sensory organ, the ocellus, has appeared and darkened. In this photograph, the adhesive papillae that extend from the head are visible under the tail to the right. These are used to adhere to a site for metamorphosis.

neural tube is completely closed and the tail elongates sufficiently to be distinguished from the head. Tailbud (Fig. 1; TBud, 20 h) begins when the tail has extended sufficiently to begin to curl within the chorion. Mid-extension stage (Fig. 1; MExt, 22 h) occurs when the tail has curled around to meet the head within the chorion. The next two stages are defined by the appearance of the otolith (24 h), a sensory organ on one side of the head, and its subsequent darkening (Fig. 1; DOtol, 26 h). Full extension of the tail (28 h) is complete when it curls one and a half times within the chorion. The tail muscles occasionally twitch at this stage. The next stage (30 h) begins with the appearance of a light sensing organ, the ocellus, which forms on the same side of the head as the otolith. The darkening of the ocellus just before hatching marks the beginning of the pre-hatching stage (Fig. 1; PreH, 32 h). This stage lasts somewhat longer than 2 h and, given the time for actual hatching of the majority of embryos in a given batch, we define the hatched stage as 36 h. This marks the end of embryonic development.

RESULTS

In the sections below, we present voltage-clamp analysis of inward and outward K^+ currents and inward Ca^{2+} currents, as well as current-clamp analysis of the action potential, at each of the eleven stages defined above (see Methods and Fig. 1). All staging was done according to these morphological criteria, and then converted into times after fertilization based on the mean chronology at 12 °C. The time axes of all figures are labelled according to these times. This eliminates the inaccuracy introduced into purely chronological staging by temperature variations and differences in the rates of development of different batches of embryos.

Development of Ca^{2+} currents

Ca^{2+} currents (I_{Ca}) were recorded from 107 cells between late gastrula and the hatched tadpole. The developmental changes that occur during this time are summarized in Fig. 2. At the neurula stage (16 h), a high-threshold inactivating I_{Ca} appears in the cells. This current activates at about −10 mV, peaks at +20 mV, and inactivates during prolonged voltage pulses by a mechanism dependent on Ca^{2+} entry (see Simoncini & Moody, 1991; Davis *et al.* 1995). During the next 4 h, I_{Ca} density rises to a value of 5·3 ± 0·8 pA pF^{-1} (20 h; measured at +20 mV), then remains almost unchanged for approximately 6 h (to 6·9 ± 1·0 pA pF^{-1} at 26 h), and subsequently increases rapidly to a final value of 26·4 ± 3·0 pA pF^{-1} in the mature cell (36 h; Fig. 2*A* and *B*). During this time, the waveform of I_{Ca} changes from inactivating to sustained (Fig. 2*A*). Between 16 and 24 h, the sustained

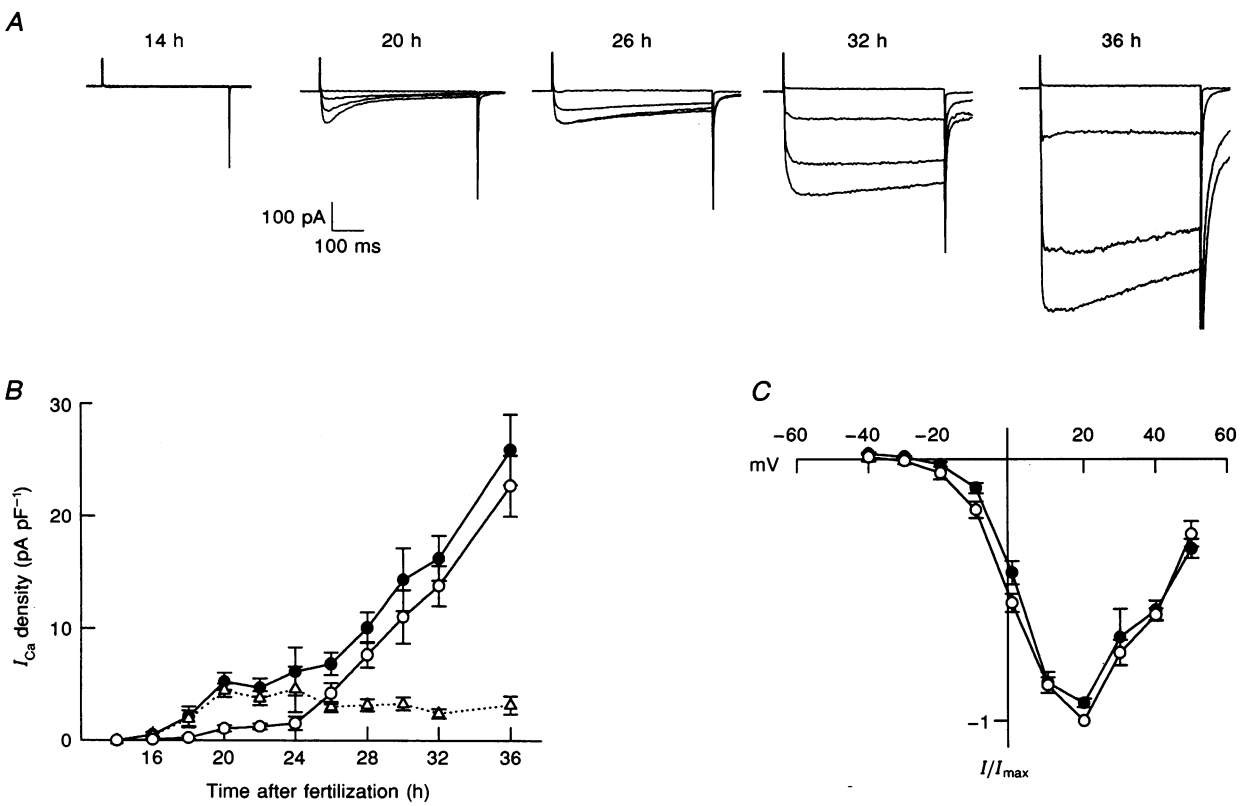

Figure 2. Development of the calcium current

A, records of I_{Ca} from 5 developmental stages from late gastrula (14 h) to the tadpole (36 h). Cs^+ internal solution was used. The holding potential was −60 mV, and currents are shown for pulses to −50, −10, 0 and +20 mV. These records have not been leak subtracted. *B*, plots of total I_{Ca} density (●; measured at +20 mV), and the inactivating (△) and sustained (○; 500 ms) components *vs.* developmental time; *n* values starting at 14 h: 4, 5, 6, 14, 10, 6, 11, 12, 8, 11 and 20. *C*, averaged normalized current *vs.* voltage relations for the inactivating (○, 20 h) and sustained (●, 36 h) forms of I_{Ca} ($n = 9$ for 20 h, $n = 20$ for 36 h; means ± S.E.M.).

component comprises 21 ± 2% of the total current ($n = 44$), whereas at 36 h it comprises 84 ± 3% ($n = 17$). The development of the total I_{Ca} and its inactivating and sustained components are plotted in Fig. 2*B*. These plots show that the inactivating component reaches its peak density at 20 h and then remains almost unchanged throughout the rest of development (values at 20 h and 36 h are not significantly different, $P = 0{\cdot}24$). In contrast, the sustained component begins to rise rapidly in density at 24 h and contributes all of the total increase in I_{Ca} after that time.

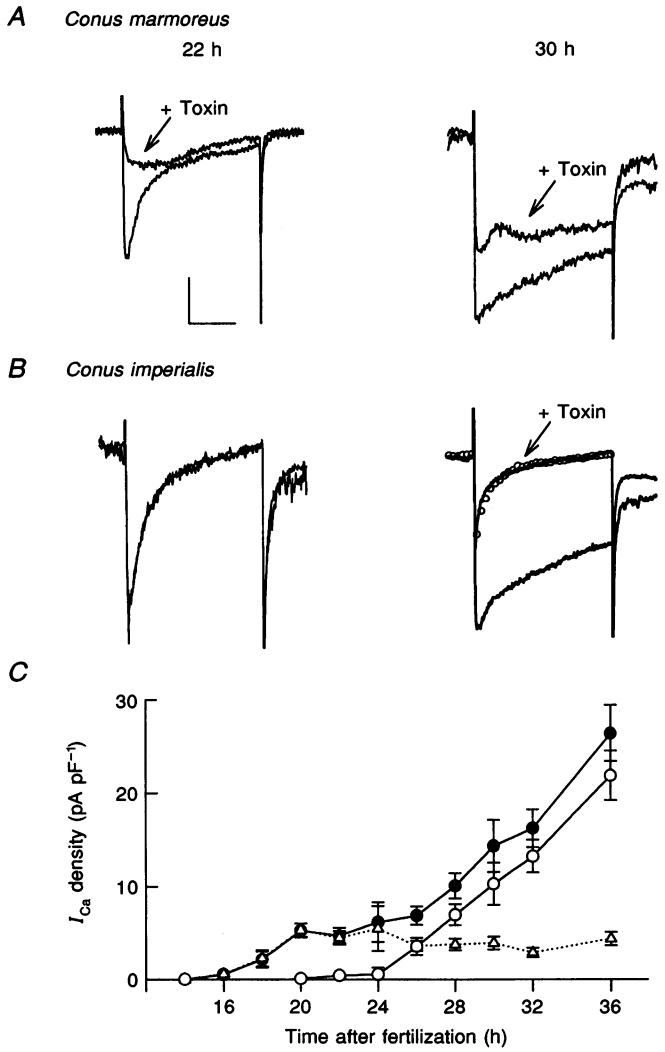

Figure 3. Separation of inactivating and sustained forms of I_{Ca} and their developmental time courses

A and *B*, effect of *Conus* toxins on the inactivating and non-inactivating forms of I_{Ca}. *A*, effect of crude toxin from *Conus marmoreus* on I_{Ca} at early (22 h) and late (30 h) stages. This toxin blocks the inactivating component of I_{Ca} at both times, even though this component is a much larger fraction of the total current at early stages. *B*, effect of crude toxin from *Conus imperialis* on I_{Ca} at early and late stages. This toxin blocks the sustained component of I_{Ca}, and thus has almost no effect at early stages; records at 22 h with and without toxin superimpose. ○ shows the current from 22 h normalized to the same peak amplitude as the current at 30 h in toxin to show the similarity of kinetics with the toxin-resistant component at 30 h. Crude toxins were applied at a concentration of 0·5 mg ml^{-1}. Calibration bars: 100 ms for all traces; 20 pA for records at 22 h; 25 pA for *A*, 30 h; 50 pA for *B*, 30 h. *Conus imperialis* toxin effect was reversible; *Conus marmoreus* was not. *C*, development of total I_{Ca} (●) and its inactivating (△) and sustained (○) subtypes. The inactivating current was taken as the difference between peak and steady-state current (500 ms) multiplied by 1·21. This figure is derived from the 79% inactivation of the current at 16–24 h, which we assume to represent a single channel type (see text). The sustained current was taken as the current at 500 ms minus the inactivating current multiplied by 0·21. Note that the sustained current first appears at 26 h, and contributes all of the increase in total current density after that time; *n* values same as in Fig. 2*B*. Records in *A* and *B*, and densities in *C* taken at +20 mV from a holding potential of −60 mV.

Although the I–V relations of the currents at 20 and 36 h are the same (Fig. 2*C*), the different sensitivities of the inactivating and sustained forms of I_{Ca} to conotoxins suggest that they are mediated by different channel types. Crude toxin from *Conus marmoreus*, a mollusc predator, preferentially blocked the inactivating component of the I_{Ca}, at both early and late stages of development (Fig. 3*A*). The block of the inactivating component was 64 ± 4%; block of the sustained component was 11 ± 24% ($n = 7$, $P = 0{\cdot}02$; measured at different developmental stages – the fractional block of each component was not stage dependent). Crude toxin from *Conus imperialis*, an annelid predator, preferentially blocked the sustained component (Fig. 3*B*). Block of the sustained component was 54 ± 8%; block of the inactivating component was 6 ± 3% ($n = 10$, $P = 0{\cdot}001$). At late stages, the component resistant to *Conus imperialis* toxin has similar kinetics to the total Ca^{2+} current at early stages (Fig. 3*B*, ○).

The developmental time courses in Fig. 2*B* were calculated assuming 100% inactivation of the inactivating component. Figure 3*C* shows a separation based on the assumption that the current that appears at 18 h represents a single channel type which shows 79% inactivation during the 500 ms test pulse. This assumption is consistent with the fact that the small Ca^{2+} current present in the oocyte, which is identical in many properties to the Ca^{2+} current in 18 h muscle cells, also shows a sustained component of about 20% (Simoncini & Moody, 1991). This separation shows that the inactivating component appears at 16 h, reaches its peak density at 20 h, and retains that density throughout the rest of development. The sustained component appears at 26 h and contributes all of the increase in total I_{Ca} density after that time. Whichever separation is correct, the results indicate that (1) the loss of inactivation during development is caused by the addition of a second Ca^{2+} channel type; (2) all of the density increase of the inactivating component occurs before 20 h; and (3) most

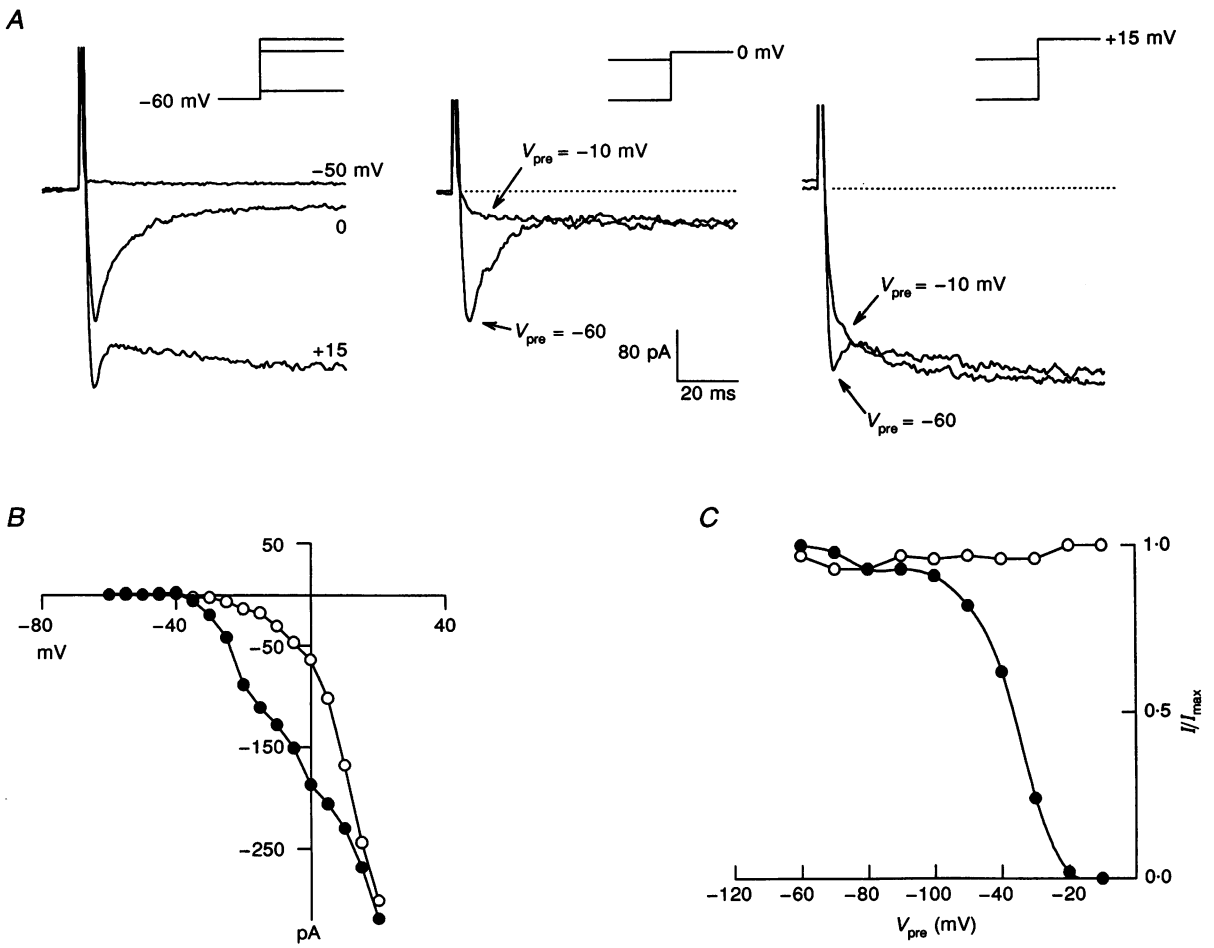

Figure 4. Low-threshold transient Ca^{2+} current

A, records from a single cell at 36 h showing the low-threshold transient Ca^{+} current. Left: currents recorded at the potentials indicated from a holding potential of −60 mV, showing that the low-threshold component dominates the records at 0 mV, whereas both components are visible at +15 mV. Middle and right: the low-threshold transient component is inactivated by a prepulse (V_{pre}) to −10 mV, whereas the sustained, high-threshold component is unaffected. *B*, I–V relations for the peak (●) and steady-state (○) currents from this cell. *C*, inactivation *vs.* addition of prepulse voltage relations for the low-threshold transient current (●, 0 mV) and the high-threshold sustained current (○, +15 mV), taken from this cell.

of the density increase of the sustained component occurs after 24 h.

A low-threshold, rapidly inactivating I_{Ca} (low-voltage-activated (LVA) or T-type) was detected in roughly 50% of the cells at each stage of development. This current was distinguishable from both the inactivating and sustained high-threshold Ca^{2+} currents by its negative voltage of activation and rapid, voltage-dependent inactivation. The LVA Ca^{2+} current increases in density during development, although its small size precluded a detailed analysis. Figure 4 shows records of this current from a tadpole muscle cell. The LVA I_{Ca} activated at about −30 mV (Fig. 4*B*), and could be inactivated completely by prepulses to −10 mV (Fig. 4*C*). These potentials are more positive than is typical of LVA Ca^{2+} currents in mammalian cells (Narahashi, Tsunoo & Yoshii, 1987). The LVA I_{Ca} may serve both to lower the threshold for spike generation and to speed the activation of the total inward current. As indicated in Fig. 4*B*, the presence of the LVA current has almost no effect on the total I_{Ca} measurements in the previous figures, which were made at +20 mV.

Development of outward K^+ currents

We measured outward K^+ current density (+60 mV) in 187 cells between 16 and 36 h. The density of the total outward K^+ current increased steadily from 11·8 ± 1·8 pA pF^{-1} at 16 h to 256·2 ± 18·0 pA pF^{-1} at 36 h (Figs 5 and 6*A*). Between 24 and 28 h, the activation of the currents abruptly speeded up and acquired a more complex waveform (Fig. 5, top row). Before this change (from 16 to 24 h), K^+ current activation in 94% of the cells could be well fitted by a single, slow exponential, which increased from 65 ± 8 ms at 16 h to 90 ± 12 ms at 24 h (Fig. 6*B*; 106/113 cells; correlation coefficient, $r > 0{\cdot}99$ for all fits; measured at +60 mV). This current was unaffected by Ca^{2+} removal (Fig. 5), and therefore we assume it is a voltage-gated K^+ current (I_K). However, after 26 h, K^+ current activation could be well fitted by a single exponential in only 17% of the cells (15/90). This was due to the addition of a rapidly activating component, which appeared in many cells as a transient on the rising phase of the current (see Fig. 5, top row, 28 h), and which in the tadpole contributes more than 50% of the total current at +60 mV. This resulted in a decline in the fastest time constant of activation from 90 ± 12 ms at 24 h, to 8 ± 1 ms in the tadpole (36 h; Fig. 6*B*); contributing to this decline were both an increase in the percentage of cells with the fast time constant (18/24 at 26 h to 22/22 at 36 h), and a decrease in the fast time constant itself (from 19 ± 2 ms to 8 ± 1 ms).

The increase in activation rate and waveform complexity after 26 h is due to the addition of Ca^{2+}-dependent K^+ currents ($I_{K(Ca)}$; see Davis *et al.* 1995). We recorded K^+

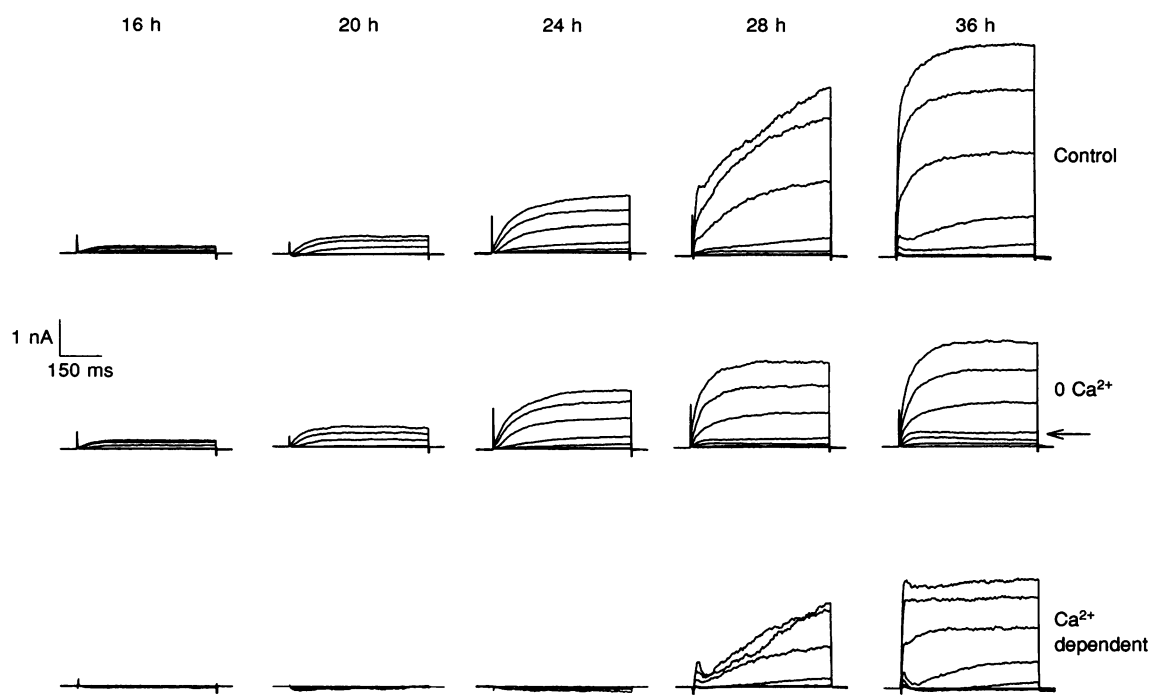

Figure 5. Development of outward K^+ currents

Outward K^+ currents recorded at 5 stages of development, in normal external solution (top row), 0 Ca^{2+} (middle), and the Ca^{2+}-dependent component derived by subtraction (bottom). These records show the late appearance of the Ca^{2+}-dependent K^+ current (see 28 and 36 h), and its rapid activation kinetics compared with the voltage-dependent K^+ current (24 h and earlier). Visible in the 0 Ca^{2+} traces at 36 h is a small residual Ca^{2+}-dependent K^+ current not blocked in 0 Ca^{2+} solution (arrow), which may represent $I_{K(Ca)}$ activated by voltage in the absence of Ca^{2+} entry.

currents in both normal and Ca^{2+}-free external solutions from fifty-four cells between 16 and 36 h. In contrast to its lack of effect at earlier stages, Ca^{2+} removal after 26 h reduced current amplitude and virtually eliminated the fast-activating components, leaving only a slowly activating current with voltage dependence and kinetics similar to I_K present at earlier stages (Fig. 5). The results of these experiments are analysed in Fig. 6*B–D*. Between 16 and 24 h, the activation time constant in 0 Ca^{2+} is not significantly different from that measured in control solution (Fig. 6*B*). After 24 h, the fastest time constant in control solutions gradually decreases by more than 10-fold, while the time constant in 0 Ca^{2+} remains slow and falls along the predicted developmental time course for I_K (Fig. 6*B*). Figure 6*C* compares the average $\tau-V$ relation for cells at 24 h in normal external solution (●) with that of the slow component remaining in 0 Ca^{2+} solution in a mature (36 h) cell. The two relations are not significantly different ($P > 0{\cdot}4$

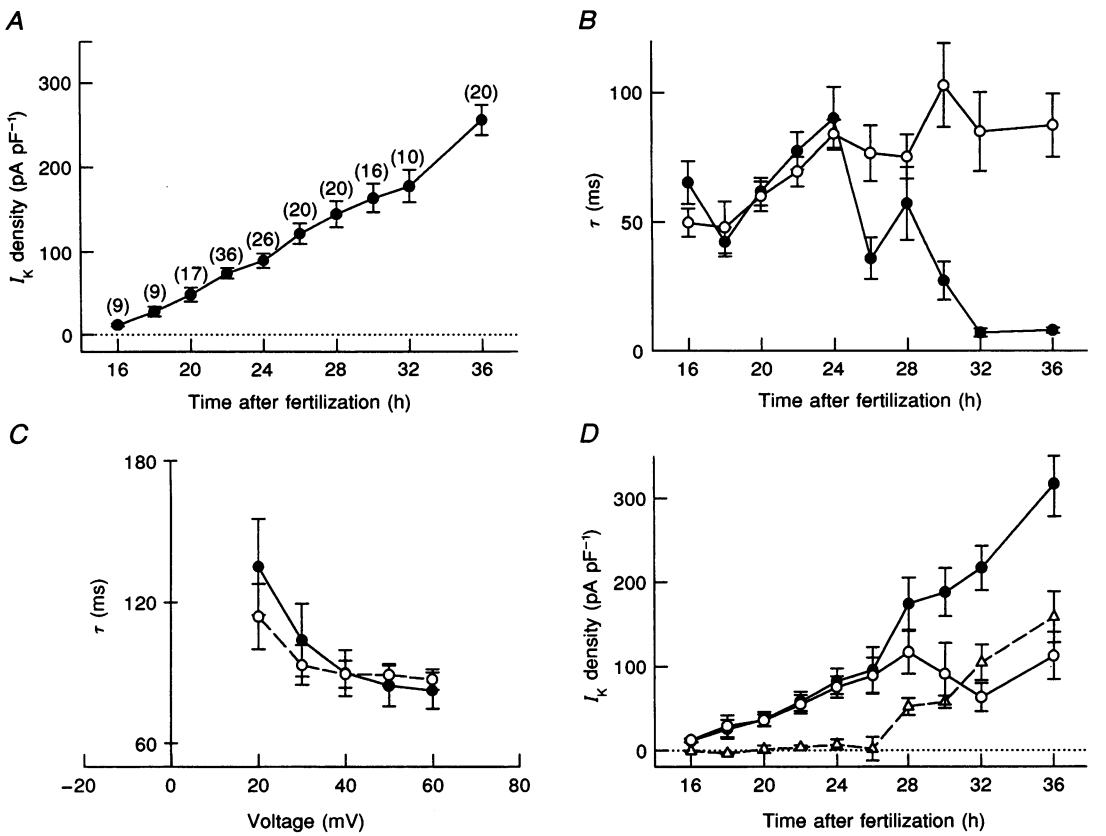

Figure 6. Development of outward K^+ current components

A, total outward K^+ current density (+60 mV) plotted *vs.* developmental time; *n* values are shown in parentheses. In *A* and *D*, K^+ current density was measured at +60 mV, where the *g vs. V* relation is saturated. *B*, activation kinetics of the total outward K^+ current. ●, the fastest time constant (+60 mV) measured in ASW plotted *vs.* developmental time. For fit analysis, no more than two time constants were used for any cell and a kinetic component had to contribute at least 10% of the total current to be accepted; *n* values same as in *A*. ○, the slow time constant measured in 0 Ca^{2+} solution is plotted *vs.* developmental time. In 100% (30/30) of the cells before 26 h, and in 50% (10/20) of the cells 26 h and later, this was the only time constant in 0 Ca^{2+}; *n* values same as in *D* (see below). *C*, average τ *vs. V* relations for the K^+ current at 24 h (●, $n = 9$) and for the slow K^+ current in 0 Ca^{2+} at 36 h (○; $n = 7$). The two relations are not significantly different at any voltage. *D*, development of the total outward K^+ current (●), and its voltage-dependent (○) and Ca^{2+}-dependent (△) components. These plots are from the subset of the cells used in panel *A*, which were exposed to both control and 0 Ca^{2+} solutions; *n* values starting at 16 h: 5, 3, 6, 8, 7, 4, 9, 5, 5 and 4. The Ca^{2+}-dependent K^+ current was measured as the difference current between control and 0 Ca^{2+} solutions (as in Fig. 5). The reduction in total current by Ca^{2+} removal was significant from 28–36 h ($P < 0{\cdot}01$), and not at any earlier stages ($P > 0{\cdot}14$). The error introduced by elimination of I_{Ca} in 0 Ca^{2+} was < 5% at +60 mV, where K^+ currents were measured (see Fig. 2). The voltage-dependent component was measured as the current in 0 Ca^{2+} in cells in which activation of this current could be fitted by a single exponential (100% at 26 h and earlier; 50% after 26 h) or, in cells which required two exponentials to fit, as the amplitude of the slower exponential component. Thus the residual $I_{K(Ca)}$ in 0 Ca^{2+} (see text) is not included in either the voltage- or Ca^{2+}-dependent components, but is included in the total K^+ current plot.

at all potentials): the current is first detectable at +10 mV and activates slowly ($\tau \approx 120$ ms); speed of activation increases with more positive potentials; and the relation saturates near +60 mV ($\tau \approx 80$ ms).

The above data indicate that I_K, which is the only outward current present before 24 h, is retained throughout later development in essentially unchanged form, and that the faster, $I_{K(Ca)}$ is simply added to it. Addition of the $I_{K(Ca)}$ both speeds activation of the total outward current by about 10-fold, and lowers its threshold of activation by 30 mV, from +10 to −20 mV. Separation of the total outward current into I_K and $I_{K(Ca)}$ reveals that I_K attains its final density at 26–28 h, the same time at which $I_{K(Ca)}$ first appears. $I_{K(Ca)}$ contributes all of the density increase in total outward current after 26 h (Fig. 6*D*). This pattern is similar to that of the two Ca^{2+} current components (see Fig. 3*C*).

Development of the composite currents of the action potential

The combination of the increased amplitude of the outward current, its increased rate of activation, and the negative shift in its voltage dependence causes a dramatic decrease in the duration of the net inward current during voltage-clamp pulses, from 134 ± 40 ms at 20 h ($n = 15$) to 8 ± 1 ms at 36 h ($n = 13$) (measured at +10 mV, using K^+ internal solution; Fig. 7). The decrease in duration of the net inward current not only has the expected effect of shortening the duration of the action potential (see Fig. 9 below), but is also likely to change the response of the cells to depolarizing stimuli. At early stages, the long duration of the net inward current would make the cells able to generate action potentials in response to slow depolarizations, whereas in the mature state, very rapid depolarizing stimuli would be required to generate action potentials, because net outward current would be generated at all potentials during a slow ramp depolarization.

Development of the inwardly rectifying K^+ current

The inwardly rectifying K^+ current ($I_{K(IR)}$) activates at potentials negative to −60 mV, and represents the major resting conductance of many oocytes and embryonic cells (see Hagiwara & Jaffe, 1979; Moody, 1995). Because it deactivates with small depolarizations, $I_{K(IR)}$ allows cells both to maintain a stable resting potential and to generate large action potentials with only small ion fluxes when stimulated (see Hille, 1992). Expression of $I_{K(IR)}$ in *Boltenia* muscle follows a pattern very different from those of the outward K^+ currents and I_{Ca} (Fig. 8). $I_{K(IR)}$ is present in the oocyte before fertilization, and is retained in the muscle lineage (and other cells) through the end of gastrulation (14 h) at approximately constant density (Block & Moody, 1987; Simoncini *et al.* 1988). This represents a substantial upregulation of the total current, because the overall surface area of the embryo increases approximately 6-fold between fertilization and gastrulation. At the end of gastrulation, the density of $I_{K(IR)}$ is 3·9 ± 1·0 pA pF^{-1} ($n = 11$). At

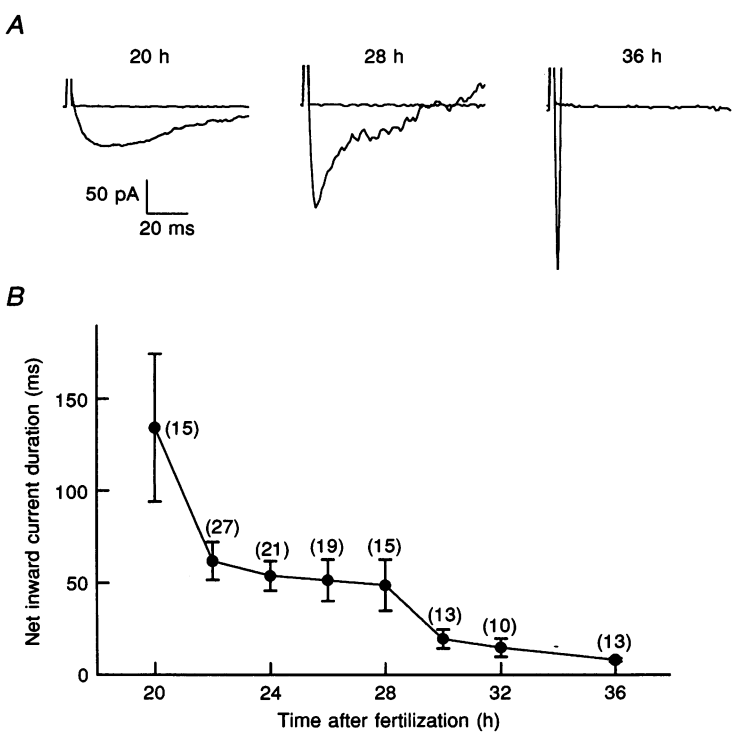

Figure 7. Developmental changes in the duration of the net inward current

A, records of net inward current (+10 mV) at 3 stages. Pipette contained K^+ internal solution. *B*, plot of the duration of the net inward current *vs.* developmental time. Duration was measured from the onset of the voltage pulse to the point at which the current crossed the zero current level (leak subtracted); *n* values in parentheses.

16 h, $I_{K(IR)}$ density decreases abruptly, reaching 0·5 ± 0·2 pA pF^{-1} ($n = 18$) by 20 h. At 22 h, $I_{K(IR)}$ density rises again, and in 6 h reaches a value not significantly different from that before its disappearance (4·1 ± 1·1 pA pF^{-1} at 26 h; $n = 20$). This density is then maintained throughout the rest of development. The currents before and after disappearance show similar voltage dependence, kinetics and pharmacology.

The fraction of cells that do not express any detectable $I_{K(IR)}$ (e.g. Fig. 8*A*, 20 h) rises from 0% at 12 h, to 33% at 16 h, to 72% at 20 h, and then gradually returns to 0% at 30 h. When these cells are excluded from the analysis, $I_{K(IR)}$ density never falls below 30% of its value at gastrula, and the period during which $I_{K(IR)}$ density is significantly decreased at all is only 4 h (18–20 h, inclusive), as opposed to 8 h (16–22 h) in the composite densities in Fig. 8*B*. These data raise two possibilities: (1) every muscle cell loses $I_{K(IR)}$ completely for a brief period (2–4 h), and the longer window of decreased mean density reflects asynchrony in times at which this total loss occurs in different cells; or (2) some cells never lose $I_{K(IR)}$.

The muscle-lineage cells possess little, if any, resting conductance other than $I_{K(IR)}$. The input resistance of cells expressing $I_{K(IR)}$ is very high (> 1 GΩ), comparable to the seal resistance, when measured between −40 mV and −60 mV (potentials at which $I_{K(IR)}$ is not activated), or at potentials negative to −60 mV in the presence of sufficient external Ba^{2+} to block $I_{K(IR)}$. During the transient absence of $I_{K(IR)}$, no new conductance appears at the resting potential. As discussed below, this transient absence of resting conductance destabilizes the resting potential, and is co-ordinated with developmental changes in I_{Ca} and outward K^+ currents to create a period during which long-duration, Ca^{2+}-dependent action potentials occur spontaneously.

Development of the action potential

Current-clamp recordings were made from fifty-eight cells between 16 and 36 h, using the perforated patch technique (see Methods). Cells at all of these stages were capable of generating action potentials in response to applied current, indicating that the input resistance of the cells at potentials positive to −60 mV, where $I_{K(IR)}$ is deactivated, is sufficiently high that even the small I_{Ca} present at early stages can support regenerative activity. Figure 9*A* shows action potentials recorded in response to applied current pulses at three stages of development. As expected from the voltage-clamp data, there was a progressive decrease in duration of about 8-fold during development (Fig. 9*B*; see also Davis *et al.* 1995), and a corresponding increase in the rates of rise and fall. The change in spike duration is gradual, and much of the decrease occurs between 16 and 24 h, before $I_{K(Ca)}$ appears. This reflects the importance of increasing K^+ current density, as well as activation rate, in controlling spike waveform (Lockery & Spitzer, 1992).

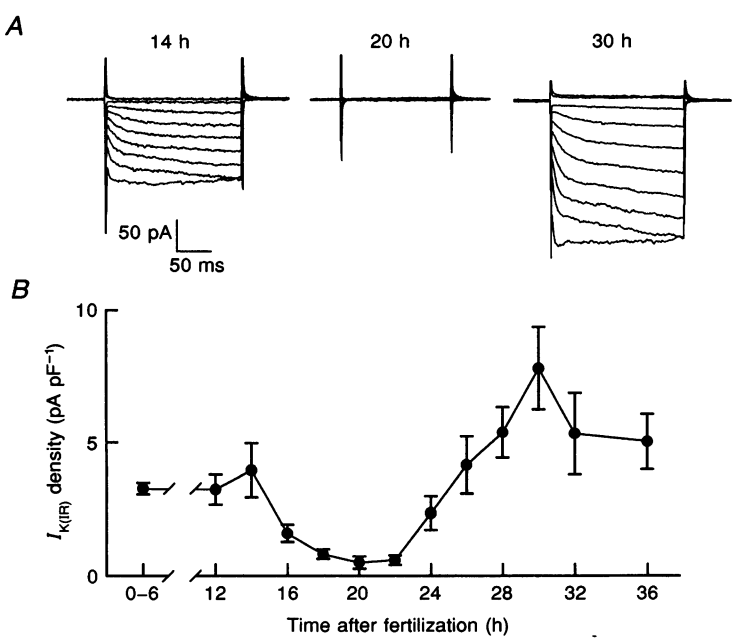

Figure 8. Development of the inwardly rectifying K^+ current

A, currents recorded from cells at 3 developmental stages at potentials of −40 to −140 mV (10 mV steps, excluding −60 mV) from a holding potential of −60 mV. *B*, plot of inward rectifier density *vs.* developmental time. The first point represents the combined mean density in the unfertilized egg, 2-, 4- and 8-cell stages. Note the break in the time axis. Density was measured at −140 mV. Cell number for the 13 data points in *B* were (starting at 0–6 h): 28, 8, 11, 21, 18, 18, 34, 22, 20, 16, 13, 6 and 15. Tested against the mean density at 0–14 h, the densities at 16–22 h are significantly reduced ($P = 0{\cdot}00002$–$0{\cdot}05$).

We also categorized the occurrence of spontaneous action potentials in the absence of applied current during whole-cell recording in 39 cells (see Fig. 9 legend for details). Figure 9*C* shows that during the time when $I_{K(IR)}$ was present only at low density (16–24 h), 85% of the cells (22/26) generated spontaneous action potentials at a frequency of $>0{\cdot}2\ s^{-1}$. After $I_{K(IR)}$ returned to control density (26–36 h), only 38% of the cells (5/13) were active, and all of those were recorded between 26 and 30 h. To guard against artifacts resulting from leakage currents at the pipette seal contributing to these measurements, we repeated the recordings using cell-attached patches, in which action potential activity can be readily monitored (see Forda, Jessell, Kelly & Rand, 1982), and obtained similar results.

DISCUSSION

A summary of the development of Ca^{2+} and K^+ currents from the unfertilized egg to the fully mature, contractile muscle is shown in Fig. 10. These density plots reveal that the patterns of channel expression during the cleavage stages (egg through neurula; 0–16 h) are very different from those during terminal differentiation (neurula through tadpole; 16–36 h). During the latter period, there are several transition points characterized by a high degree of co-ordination among the functional expression of different channel types.

During the cleavage stages, currents present in the oocyte are sequentially lost, each at a specific stage, and no new currents appear. The Na^+ current (not shown in Fig. 10) present in the unfertilized egg disappears completely by first cleavage, 2 h after fertilization (Block & Moody, 1987). A high-threshold inactivating I_{Ca} is also present in the oocyte, very similar to that just after neurulation, but at about 10-fold lower density (mean $0{\cdot}5\ pA\ pF^{-1}$; see Simoncini & Moody, 1991). It is maintained at constant density through the 32-cell stage (not visible at the scale used in Fig. 10), a process which requires upregulation of the total I_{Ca} due to the addition of substantial new membrane to the embryo, and then disappears entirely before gastrulation (12 h; Simoncini *et al.* 1988; Simoncini & Moody, 1991). $I_{K(IR)}$ follows a similar pattern to I_{Ca}, but disappears later, after neurulation (16 h).

The downregulation of $I_{K(IR)}$ begins very close to the time of the last cell division in the muscle lineage (Satoh, 1994), marking the onset of terminal differentiation, and within

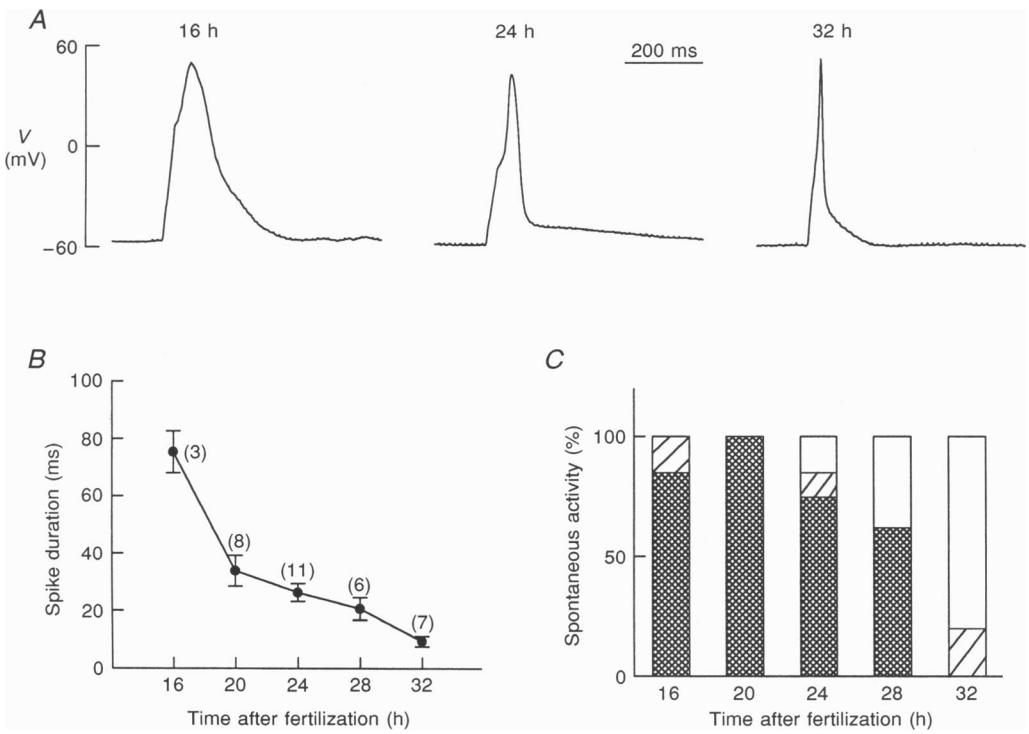

Figure 9. Development of the action potential and spontaneous activity

A, records of action potentials elicited by brief current pulses at 3 developmental stages. *B*, plot of action potential duration (at +20 mV) *vs.* developmental time; *n* values in parentheses. *C*, plot of the occurrence of spontaneous action potentials at 5 developmental stages. After establishing whole-cell configuration in perforated patch mode, action potential frequency was measured for a minimum of 10 s. Cells were classified as follows: ▩, action potential frequency $>0{\cdot}2\ s^{-1}$; ▨, action potential frequency $<0{\cdot}1\ s^{-1}$ or oscillations of membrane potential positive to −50 mV; □, stable membrane potential negative to −50 mV with no action potentials; *n* values same as in *B*. Voltage-clamp records were taken from each cell to confirm that I_K and $I_{K(IR)}$ densities and kinetics were as expected from the morphological staging.

2 h of the appearance of two other currents: (1) a high-threshold inactivating I_{Ca}, similar to that found in the oocyte, but which now increases within 4 h to a density 10-fold higher than in the oocyte (Fig. 10*A*, hatched curve); and (2) a slowly activating voltage-dependent outward K^+ current, which was never seen at earlier stages (Fig. 10*B*, hatched curve). Approximately 6 h later, at tailbud stage, $I_{K(IR)}$ reaches its minimum density and the inactivating form of I_{Ca} reaches its maximum density. At this time, although the outward K^+ current has increased in density, it is still composed entirely of the voltage-dependent component, which is high threshold and slowly activating. Approximately 6 h after $I_{K(IR)}$ reaches its minimum density, three events occur within 2 h of each other: (1) $I_{K(IR)}$ density returns to its pre-disappearance value; (2) the sustained Ca^{2+} current begins its major increase in density (Fig. 10*A*, filled curve); and (3) $I_{K(Ca)}$ first appears, adding a rapidly activating, low-threshold component to the outward current (Fig. 10*B*, filled curve).

These data show that the development of the channels that mediate the action potential is co-ordinated with that of the channels that set the resting potential to create a period of spontaneous activity. During this time, the absence of $I_{K(IR)}$ destabilizes the resting potential, the presence of I_{Ca} ensures that there is sufficient inward current to drive the rising phase of the action potential, and the slow activation and high threshold of I_K allows for long-duration action potentials and ensures that action potenials can be triggered

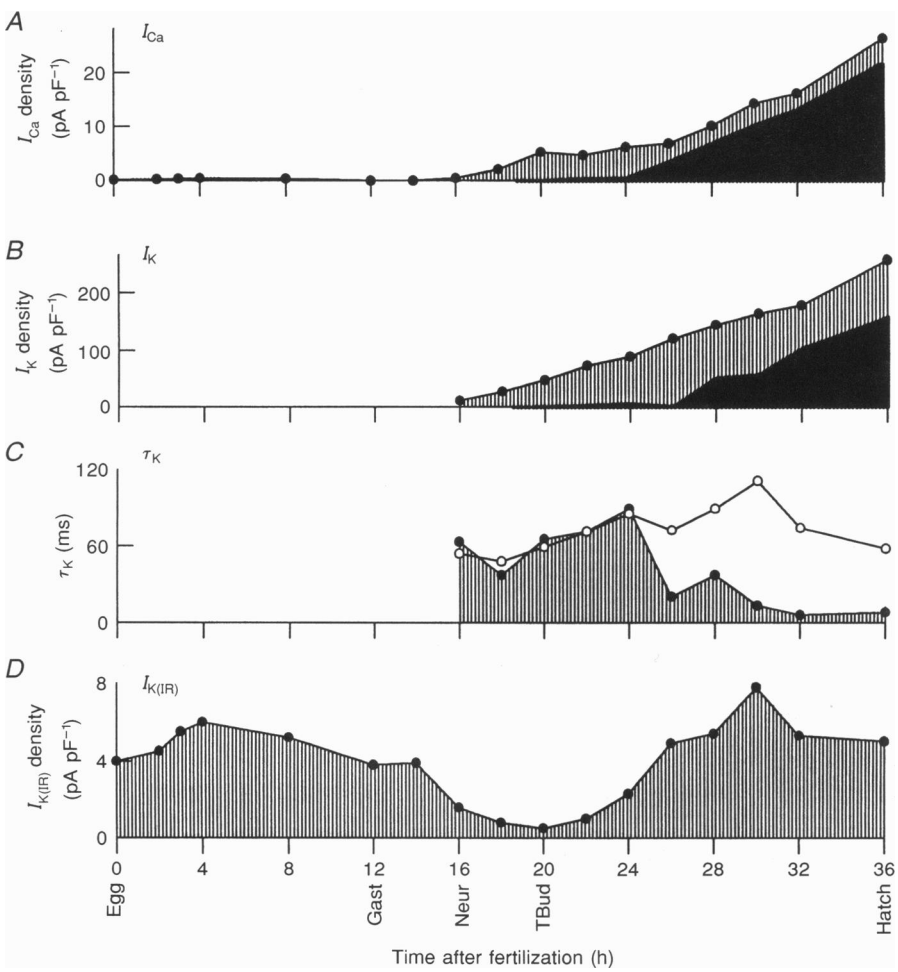

Figure 10. Summary of the development of Ca^{2+} and K^+ currents in ascidian muscle

Note that the plots start at fertilization; data before gastrula (12 h) is from muscle-lineage cells whose descendants also include non-muscle cells. *A*, total Ca^{2+} current density and its inactivating and sustained components; total density is indicated by ●, vertical hatching indicates the inactivating component, and the filled plot the sustained component. Values at 0–8 h are approximately 0·5 pA pF^{-1}; values at 12 and 14 h are 0. *B*, total K^+ current density (●) and its voltage-dependent (hatched) and Ca^{2+}-dependent (filled) components. The small Ca^{2+}-dependent component before 26 h probably reflects an effect of 0 Ca^{2+} solution on the voltage-dependent K^+ current, because these currents showed no fast kinetic component. *C*, activation kinetics of the total outward K^+ current: ● (hatched curve), the fastest time constant measured in ASW; ○, the slow time constant measured in 0 Ca^{2+} solution. In 100% (30/30) of the cells before 26 h, and in 50% (10/20) of the cells 26 h and later, this was the only time constant in 0 Ca^{2+}. *D*, inward rectifier density.

by slow depolarizing events. The window of spontaneous activity is terminated by two events: (1) $I_{K(IR)}$ density increases sufficiently to stabilize the resting potential; and (2) the $I_{K(Ca)}$ density increases enough so that action potentials are unlikely to be triggered by slow, spontaneous depolarizations.

All of these changes occur in the absence of innervation, in cells cultured from neurula-stage embryos (18 h). Muscle cells acutely dissociated from hatched tadpoles show very similar properties, indicating that innervation *in vivo* probably does not play a major role in channel development, although it may influence the timing with which various currents appear. It is not known exactly when innervation occurs in this species, although we first see spontaneous muscle contractions in intact embryos at 28 h. This corresponds approximately with the stage at which spontaneous junctional potentials are first recorded in other ascidians (Ohmori & Sasaki, 1977), indicating that functional neuromuscular contacts may be formed during the latter part or just after the window of spontaneous activity.

Thus the inactivating Ca^{2+} current and the slow, voltage-dependent K^+ current, which appear at the same time, represent ion channels which function primarily in the immature muscle cell, before the development of contractility, to mediate long-duration action potentials. These action potentials occur spontaneously because of the virtual absence of the inward rectifier. Ca^{2+} entry during these action potentials appears to be necessary for the later development of $I_{K(Ca)}$ (Dallman, Greaves, Davis & Moody, 1995). The sustained Ca^{2+} current and the rapidly-activating $I_{K(Ca)}$, on the other hand, function in the mature cells. They mediate a short-duration action potential which, because of the reappearance of the inward rectifier, occurs only when triggered by synaptic input and serves to mediate contraction. The immature currents are retained in the mature cell, although their function is not clear.

Although the appearance of I_{Ca} and I_K, and the disappearance of $I_{K(IR)}$ all occur near the time of withdrawal of the muscle-lineage cells from the cell cycle, they are probably regulated differently. The appearance of I_{Ca} and I_K requires a preceding period of RNA synthesis which extends several cell cycles earlier than the terminal one, whereas the disappearance of $I_{K(IR)}$ does not (Simoncini & Moody, 1991). Furthermore, I_{Ca} and I_K appear first in muscle-lineage cells and only later, if at all, in other cell types, whereas $I_{K(IR)}$ disappears in all cell types simultaneously (Simoncini *et al.* 1988). Because the inward rectifier is the last in a sequence of three oocyte channel types to disappear, and because the disppearance of the first one, the oocyte Na^+ channel, is linked to the cell-cycle clock (Coombs, 1995), $I_{K(IR)}$ loss might also be regulated by the cell cycle. The entire window of time when $I_{K(IR)}$ density is low could be regulated in this way if withdrawal from the cell cycle triggered both the rapid removal of inward rectifier channels from the membrane and the slower synthesis of a mature form of the channel. Similarly, although the late appearance of $I_{K(Ca)}$ and the sustained Ca^{2+} current occur at nearly the same time, they too appear to be separately regulated. The appearance of the $I_{K(Ca)}$ is regulated by spontaneous activity, whereas that of the sustained Ca^{2+} current is not (Dallman *et al.* 1995).

The significance of the transition from an inactivating to a sustained Ca^{2+} current is not obvious. In the mature cells, the duration of the action potential is only about 10 ms, so that the behaviour of the Ca^{2+} current at longer times would not seem to be very important in determining spike waveform or Ca^{2+} entry. It is possible that the significance lies in the behaviour of the Ca^{2+} current at the termination of the action potential. At early stages, the inactivating Ca^{2+} channels may reopen on repolarization, thus increasing the amount of Ca^{2+} entry caused by each spike (Slesinger & Lansman, 1991). In the mature cells, in which action potentials occur at high frequency during swimming, the lack of inactivation may ensure that Ca^{2+} channels are available to open at the onset of each spike.

The coincidence of the appearance of the sustained Ca^{2+} current and the $I_{K(Ca)}$ raises the possibility that the developmental profile of $I_{K(Ca)}$ that we measure under voltage clamp reflects the development of sufficient Ca^{2+} entry to activate these channels rather than the development of the channels themselves. It is also possible that the subsequent speeding of activation of $I_{K(Ca)}$ reflects a change in the kinetics of Ca^{2+} entry, or in the spatial association of Ca^{2+} and Ca^{2+}-dependent K^+ channels (see Wisgirda & Dryer, 1994).

Some of these events are very similar to those in other cell types. In *Xenopus* spinal neurones, for example, the early appearance of I_{Ca} and the later speeding of delayed K^+ current activation creates a period during which action potential duration is long, and the occurrence of spontaneous action potentials during this time is responsible for some of the K^+ current speeding (Barish, 1986; O'Dowd *et al.* 1988; Desarmenian & Spitzer, 1991). However, the genesis of the spontaneous activity is not known in *Xenopus* neurones. Because spontaneous activity early in development is widespread in the vertebrate nervous system (see Shatz, 1990), it is possible that co-ordination of the development of channels that set the resting potential and those that determine ion fluxes during the action potential, such as we have reported here, is a phenomenon of general importance.

Barish, M. E. (1986). Differentiation of voltage-gated potassium current and modulation of excitability in cultured amphibian neurones. *Journal of Physiology* **375**, 229–250.

Barres, B. A., Koroshetz, W. J., Swartz, K. J., Chun, L. L. Y. & Corey, D. P. (1990). Ion channel expression by white matter glia: the O-2A glial progenitor cell. *Neuron* **4**, 507–524.

Block, M. L. & Moody, W. J. (1987). Changes in sodium, calcium and potassium currents during early embryonic development of the ascidian *Boltenia villosa*. *Journal of Physiology* **393**, 619–634.

Cerny, L. C. & Bandman, E. (1986). Contractile activity is required for the expression of neonatal myosin heavy chain in embryonic chick pectoral muscle cultures. *Journal of Cell Biology* **103**, 2153–2161.

Coombs, J. L. (1995). The cell-cycle dependent regulation of the sodium current and membrane surface area in an ascidian egg. PhD Thesis, University of Washington, Seattle, WA, USA.

Dallman, J. E., Greaves, A. A., Davis, A. K. & Moody, W. J. (1995). A role for spontaneous activity in the differentiation of muscle cells of the ascidian *Boltenia villosa*. *Society for Neuroscience Abstracts* **21**, 61.

Davis, A. K., Greaves, A. A., Dallman, J. E. & Moody, W. J. (1995). Comparison of ionic currents expressed in immature and mature muscle cells of an ascidian larva. *Journal of Neuroscience* **15**, 4875–4884.

Desarmenien, M. G. & Spitzer, N. C. (1991). Role of calcium and protein kinase C in development of the delayed rectifier potassium current in *Xenopus* spinal neurons. *Neuron* **7**, 797–805.

Dutton, E. K., Simon, A. M. & Burden, S. J. (1993). Electrical activity-dependent regulation of the acetylcholine receptor δ-subunit gene, MyoD, and myogenin in primary myotubes. *Proceedings of the National Academy of Sciences of the USA* **90**, 2040–2044.

Forda, S. R., Jessell, T. M., Kelly, J. S. & Rand, R. P. (1982). Use of the patch electrode for sensitive high resolution extracellular recording. *Brain Research* **249**, 371–378.

Hagiwara, S. & Jaffe, L. A. (1979). Electrical properties of egg cell membranes. *Annual Review of Biophysics and Bioengineering* **8**, 385–416.

Hille, B. (1992). *Ionic Channels of Excitable Membranes*, 2nd edn. Sinauer Associates, Sunderland, MA, USA.

Holliday, J. & Spitzer, N. C. (1990). Spontaneous calcium influx and its role in differentiation of spinal neurons in culture. *Developmental Biology* **141**, 13–23.

Horn, R. & Marty, A. (1988). Muscarinic activation of ionic currents measured by a new whole-cell recording method. *Journal of General Physiology* **92**, 145–159.

Jones, S. M. & Ribera, A. B. (1994). Overexpression of a potassium channel gene perturbs neural differentiation. *Journal of Neuroscience* **14**, 2789–2799.

Linsdell, P. & Moody, W. J. (1994). Na^+ channel misexpression accelerates K^+ channel development in embryonic *Xenopus laevis* skeletal muscle. *Journal of Physiology* **480**, 405–410.

Linsdell, P. & Moody, W. J. (1995). Electrical activity and calcium influx regulate ion channel development in embryonic *Xenopus* skeletal muscle. *Journal of Neuroscience* **15**, 4507–4514.

Lockery, S. R. & Spitzer, N. C. (1992). Reconstruction of action potential development from whole-cell currents of differentiating spinal neurons. *Journal of Neuroscience* **12**, 2268–2287.

Moody, W. J. (1995). Critical periods of early development created by the coordinate modulation of ion channel properties. *Perspectives on Developmental Neurobiology* **2**, 309–315.

Moody, W. J. & Bosma, M. M. (1985). Hormone-induced loss of surface membrane during maturation of starfish oocytes: Differential effects of potassium and calcium currents. *Developmental Biology* **112**, 396–404.

Moody, W. J., Simoncini, L., Coombs, J. L., Spruce, A. E. & Villaz, M. (1991). Development of ion channels in early embryos. *Journal of Neurobiology* **22**, 674–684.

Narahashi, T., Tsunoo, A. & Yoshii, M. (1987). Characterization of two types of calcium channels in mouse neuroblastoma cells. *Journal of Physiology* **383**, 231–239.

O'Dowd, D. L., Ribera, A. B. & Spitzer, N. C. (1988). Development of voltage-dependent calcium, sodium, and potassium currents in *Xenopus* spinal neurons. *Journal of Neuroscience* **8**, 792–805.

Ohmori, H. & Sasaki, S. (1977). Development of neuromuscular transmission in a larval tunicate. *Journal of Physiology* **269**, 221–254.

Satoh, N. (1994). Developmental biology of ascidians. In *Developmental and Cell Biology Series*, vol. 29. Cambridge University Press, Cambridge.

Shatz, C. J. (1990). Impulse activity and the patterning of connections during CNS development. *Neuron* **5**, 745–756.

Simoncini, L., Block, M. L. & Moody, W. J. (1988). Lineage-specific development of calcium currents during embryogenesis. *Science* **242**, 1572–1585.

Simoncini, L. & Moody, W. J. (1991). Dependence of Ca^{2+} and K^+ current development on RNA and protein synthesis in muscle-lineage cells of the ascidian *Boltenia villosa*. *Journal of Neuroscience* **11**, 1413–1420.

Slesinger, P. A. & Lansman, J. B. (1991). Reopening of Ca^{2+} channels in mouse cerebellar neurons at resting membrane potentials during recovery from inactivation. *Neuron* **7**, 755–762.

Sontheimer, H., Trotter, J., Schachner, M. & Kettenman, H. (1989). Channel expression correlates with differentiation stage during development of oligodendrocytes from their precursor cells in culture. *Neuron* **2**, 1135–1145.

Spitzer, N. C. (1991). A developmental handshake: neuronal control of ionic currents and their control of neuronal differentiation. *Journal of Neurobiology* **22**, 659–673.

Wisgirda, M. E. & Dryer, S. E. (1994). Functional dependence of Ca^{2+}-activated K^+ current on L- and N-type Ca^{2+} channels: differences between chicken sympathetic and parasympathethic neurons suggest different regulatory mechanisms. *Proceedings of the National Academy of Sciences of the USA* **91**, 2858–2862.

Acknowledgements

This work was supported by grant HD17486 to W.J.M. from the National Institutes of Health, by NIH Training Grant GM07270 to J.E.D., and by a National Science Foundation graduate fellowship to A.A.G. We especially thank Professor Baldomero Olivera at the University of Utah for kindly providing the *Conus* toxins used in this study. We thank Douglas Currie, Heidi Picken-Bahrey, and Gilles Charpentier for reading the manuscript.

Author's email address

W. J. Moody: profbill@u.washington.edu

Received 6 March 1996; accepted 14 August 1996.